JOC The Journal of Organic Chemistry

Article

pubs.acs.org/joc

Mechanisms and Origins of Selectivities of the Lewis Acid-Catalyzed Diels–Alder Reactions between Arylallenes and Acrylates

Peiyuan Yu,[†] Wei Li,[†] and K. N. Houk*

Department of Chemistry and Biochemistry, University of California, Los Angeles, California 90095, United States

Supporting Information

ABSTRACT: The mechanisms of recently reported Lewis acid-catalyzed Diels–Alder reactions of arylallenes and acrylates were studied using density functional theory calculations. A stepwise mechanism involving short-lived zwitterion intermediates is established. The reaction is *endo*-selective in the presence of Lewis acid catalyst. The [2 + 2] cycloaddition is not observed because of the greater charge separation in the first step of the [2 + 2] cycloaddition. The origins of chirality transfer in the Diels–Alder reaction using chiral arylallenes are uncovered, and the absolute stereochemistry of the product is predicted.

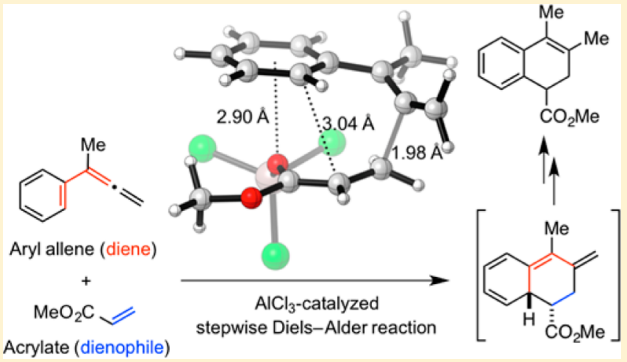

INTRODUCTION

The Diels–Alder (DA) reaction of dienes and alkenes is one of the most useful ring-forming reactions in organic chemistry.[1−5] Despite numerous advances since it was established in 1928, the scope of this powerful transformation has been continuously expanded.[6−11] Recently, in their quest to develop [2 + 2] cycloaddition reactions to synthesize cyclobutanes, Conner and Brown discovered an unexpected Lewis acid-catalyzed DA reaction of arylallenes and acrylates, involving the aromatic ring as part of the diene (Scheme 1).[12]

On the basis of their previous work,[13] the authors were expecting a [2 + 2] cycloaddition of arylallene and acrylate to produce a cyclobutane (Scheme 1a).[12] However, the observed product of the reaction between **1** and **2** is dihydronaphthalene **4** (Scheme 1b).

The observed reaction was proposed to proceed via a concerted asynchronous [4 + 2] transition state to form a dearomatized intermediate, followed by a formal 1,5-H shift to afford the final product.[12] The reaction is also suggested to follow the "*endo* rule".[14] However, the key intermediate could not be observed, and this stereochemistry could not be confirmed. We have undertaken a density functional theory (DFT) study to investigate the mechanisms and origins of product selectivity of this unusual Diels–Alder reaction. We have also explored the [2 + 2] cycloaddition reaction, to explain why it was not observed.

COMPUTATIONAL METHODS

All DFT calculations were performed using Gaussian 09.[15] Geometry optimizations and frequency calculations were performed at the M06-2X/6-31G(d) level of theory.[16] Solvent effects were modeled with the conductor-like polarizable continuum model (CPCM) using dichloromethane as the solvent.[17] Normal vibrational mode analysis confirmed

Scheme 1. Lewis Acid-Catalyzed Diels–Alder Reactions between Arylallenes with Acrylates[12]

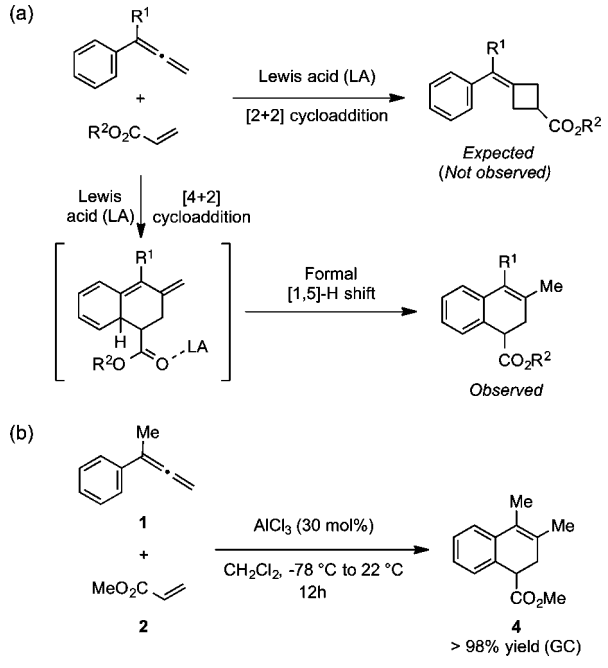

that optimized structures are minima or transition structures. Truhlar's quasiharmonic correction was used to compute molecular entropies to reduce error caused by the breakdown of the harmonic approximation, by setting all positive frequencies that are less than 100 cm^{-1} to 100 cm^{-1}.[18] CPCM(dichloromethane)-M06-2X/6-311+G(d,p) single-

Received: May 10, 2017
Published: May 16, 2017

DOI: 10.1021/acs.joc.7b01132
J. Org. Chem. 2017, 82, 6398−6402

point energies were computed on the CPCM(dichloromethane)-M06-2X/6-31G(d)-optimized structures. All 3D renderings of stationary points were generated using CYLview.[19] GaussView[20] and Avogadro[21] were used to construct initial structures used in our computations.

RESULTS AND DISCUSSION

Uncatalyzed Diels–Alder Reaction. We first studied the uncatalyzed Diels–Alder reaction between phenylallene **1** and methyl acrylate (**2**). Figure 1 shows the optimized transition

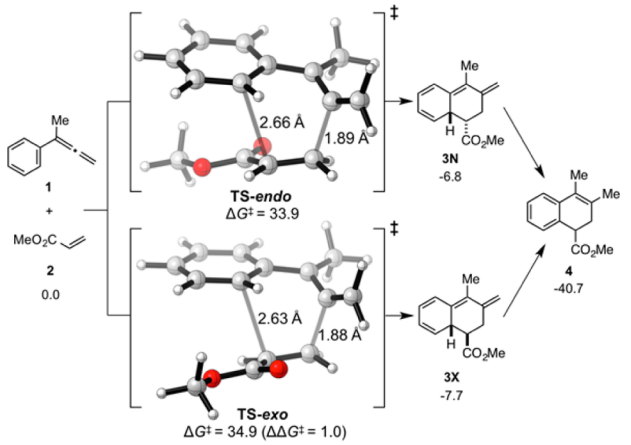

Figure 1. Transition structures and free energy profile for the uncatalyzed Diels–Alder reaction between **1** and **2**. Energies are given in kilocalories per mole.

structures (TSs) and free energy profiles for the *endo* and *exo* pathways of the reaction. Both TS-*endo* and TS-*exo* are concerted yet highly asynchronous, each with a shorter forming bond at ∼1.9 Å and a longer forming bond at ∼2.6 Å. TS-*endo* is slightly favored over TS-*exo* ($\Delta\Delta G^{\ddagger}$ = 1.0 kcal/mol), although neither process is likely to proceed at room temperature due to the high barriers of reaction (∼34 kcal/mol). The Diels–Alder adducts are about 7 kcal/mol more stable than the reactants. The formal [1,5]-hydrogen shift process is highly exergonic because of rearomatization and the formation of a more substituted alkene in the final product.

$AlCl_3$-Catalyzed Diels–Alder Reaction. The association of $AlCl_3$ with the carbonyl oxygen of **2** is highly exergonic with a computed ΔG of −25.0 kcal/mol (Figure 2). The association of $AlCl_3$ with the final product **4** is even stronger (−26.2 kcal/mol). This rationalizes the need for a relatively high amount of catalyst loading (30 mol %), since product inhibition will occur.

Figure 3 shows the optimized *endo* and *exo* transition structures, intermediates, and computed free energy profiles for the DA reactions in the presence of $AlCl_3$. The Diels–Alder

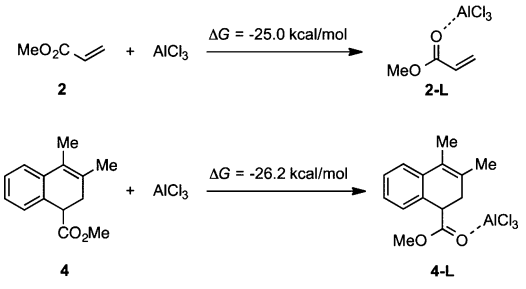

Figure 2. Energetics for the association of $AlCl_3$ with the carbonyl oxygens of **2** and **4**.

reaction is much faster with the carbonyl oxygen of the dienophile coordinated to $AlCl_3$ (**2-L**). The free energy barrier is now only 19.8 kcal/mol through the *endo* transition state (TS-1-*endo*). This corresponds to an enormous (∼10^{10}-fold) rate enhancement compared to the uncatalyzed reaction. The transition structures are also earlier in terms of forming bond lengths. There is essentially only one forming bond at ∼2.0 Å, and a stable zwitterion intermediate could be located on the potential energy surface for both the *endo* and the *exo* pathways (INT-N and INT-X). However, the intermediates are predicted to be exceedingly short-lived, with the second step to form the DA adduct being almost barrierless ($\Delta G^{\ddagger}$ = ∼1.0 kcal/mol). This is in agreement with the experimentally observed stereospecificity of the reaction using deuterium-labeled acrylate. TS-1-*exo* is 2.5 kcal/mol higher in energy than TS-1-*endo*. The catalyzed reaction is not only faster than the uncatalyzed one, but also more *endo*-selective.

$AlCl_3$-Catalyzed [2 + 2] Cycloaddition. We next investigated the mechanisms of the [2 + 2] cycloaddition of **1** and **2-L**. In principle, the [2 + 2] product could be formed via TS-1-*endo* and INT-N. However, because the second step to form the [4 + 2] product has an extremely small barrier (1.2 kcal/mol, i.e., essentially barrierless), it is possible that the [4 + 2] product could be formed directly from TS-1-*endo*, bypassing the intermediate INT-N on the potential energy surface (PES).[22] In such a case, the required conformational change (C–C bond rotation) and subsequent formation of the second C–C bond to afford the [2 + 2] product are unlikely to happen. Other evidence for the extremely short lifetime of the intermediate comes from the experimental results, where the product stereochemistry was preserved using deuterium-labeled acrylate starting materials.[12] The experimentally observed stereospecificity suggests that free rotation of C–C single bond is restricted during the lifetime of the intermediate. Therefore, we explored other conformations of the first transition state for the [2 + 2] pathway. Different approaching geometries and conformations were explored. For the formation of the first bond, 13 transition structures that are within 2 kcal/mol relative to the lowest energy TS were located (Figure S1). The lowest energy reaction pathway is shown in Figure 4.

The [2 + 2] cycloaddition of **1** and **2-L** has a free energy barrier of 24.9 kcal/mol via TS-3. The forming bond length is ∼2 Å, similar to that of the first TS of the Diels–Alder reaction. A stable zwitterion intermediate (INT) can also be obtained. However, the second step has a substantial barrier of ∼7 kcal/mol via TS-4 to form the cyclobutane. The first step is rate determining. It is 5 kcal/mol higher in energy than the first step of the DA reaction and thus is predicted not to compete with the observed Diels–Alder reaction.

Origins of the Preference of Diels–Alder over [2 + 2] Cycloadditions. To probe the origins of the *endo*-selectivity of the DA reaction and to explain why the [2 + 2] TS has a much higher barrier than the DA reaction, we analyzed the transition structures using the distortion/interaction model, also known as the activation strain model.[23] Each transition structure is separated into two fragments, followed by single-point energy calculations on each fragment. The difference in energy between the distorted fragments and optimized ground-state geometries is the distortion energy ($E^{\ddagger}_{dist}$), or the activation strain. The difference between the electronic energy of activation ($\Delta E^{\ddagger}$) and the distortion energy is the interaction energy ($E^{\ddagger}_{int}$). We have also computed the dipole moments and

DOI: 10.1021/acs.joc.7b01132
J. Org. Chem. 2017, 82, 6398–6402

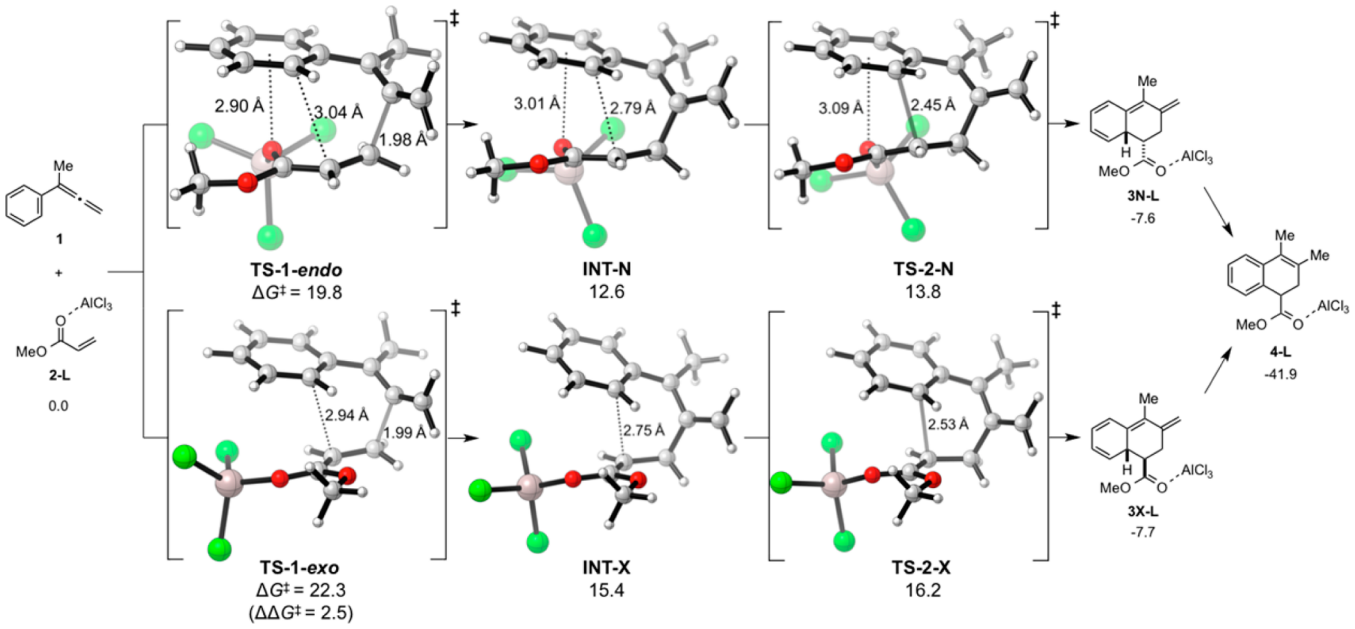

Figure 3. Transition structures, intermediates, and free energy profile for the Diels–Alder reaction between **1** and **2-L**. Energies are given in kilocalories per mole.

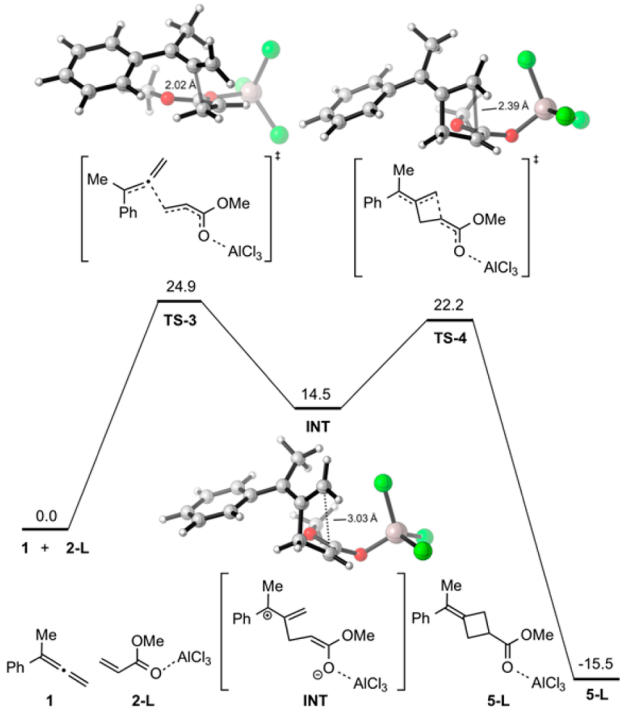

Figure 4. Transition structures, intermediate, and free energy profile for the [2 + 2] cycloaddition of **1** and **2-L**.

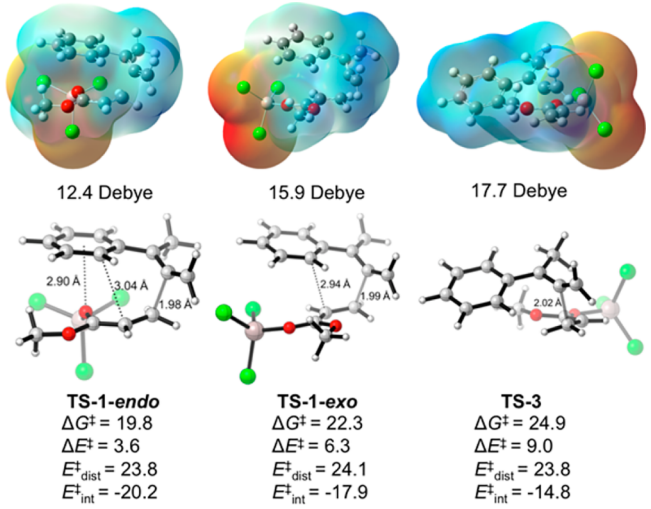

Figure 5. Electrostatic potential (ESP) maps, dipole moments, and distortion/interaction analysis of TS-1-*endo*, TS-1-*exo*, and TS-3.

plotted the electrostatic potential (ESP) maps of the transition structures. The results are shown in Figure 5.

The free energies ($\Delta G^{\ddagger}$) of TS-1-*exo* and TS-3 are higher than that of TS-1-*endo* by 2.5 and 5.1 kcal/mol, respectively. The corresponding electronic energies of activation ($\Delta E^{\ddagger}$) follow the same trend. The distortion energies are essentially identical for the three transition structures (at ~24 kcal/mol). This results from the great asynchronicity in these three structures, all of which have a forming bond length of 1.98–2.02 Å. TS-1-*endo* has the most favorable interaction energy of −20.2 kcal/mol, followed by TS-1-*exo* (−17.9 kcal/mol), while TS-3 has the least favorable interaction energy (−14.8 kcal/mol). The difference in interaction energy is due to different electrostatic interactions between the two fragments in the TS. The electronegative region (red in the ESP) in TS-1-*endo* is right below the electropositive (blue) phenyl ring, while TS-1-*exo* and TS-3 have more separation of charges. The computed dipole moments of the three TS also support this hypothesis, as they correlate with the relative energies.

Unreactive Dienophiles. One of the more unusual aspects of this reaction is the dienophiles that do not undergo reaction, as pointed out by Conner and Brown.[12] For example, a β-substituent as small as chloride (**29**) was not tolerated in the reaction. We have investigated the reaction of **29a** (the corresponding methyl ester) with **1** (Figure 6). The activation barrier is 23.1 kcal/mol (3.3 kcal/mol higher than that of TS-1-*endo*). Distortion/interaction analysis shows that there is a

DOI: 10.1021/acs.joc.7b01132
J. Org. Chem. 2017, 82, 6398–6402

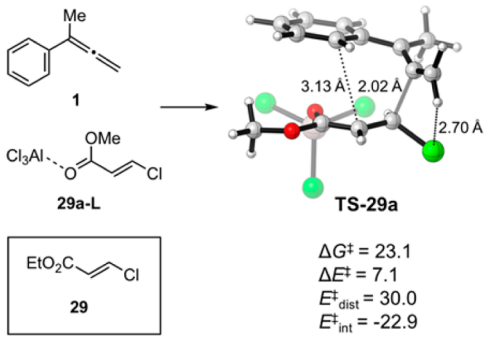

Figure 6. Transition structure (TS-29a) for the Diels–Alder reaction between **1** and **29a-L** and the corresponding distortion/interaction analysis.

much greater distortion energy (30.0 kcal/mol) in the transition structure, as compared to that of TS-1-*endo* (23.8 kcal/mol). This overrides the slightly more favorable interaction energy with the chloride substituent. Our results suggest that β-substituents (X) other than hydrogen were not tolerated because of the greater distortion energies to bend the carbon–X bond. This is a result of the highly asynchronous nature of the transition structure in the stepwise mechanism of this Diels–Alder reaction.

[1,5]-H Shift. Presumably, the concerted suprafacial [1,5]-H shift could not proceed due to the rigid diene. As shown in Figure 7, the transition structure for such a process is highly

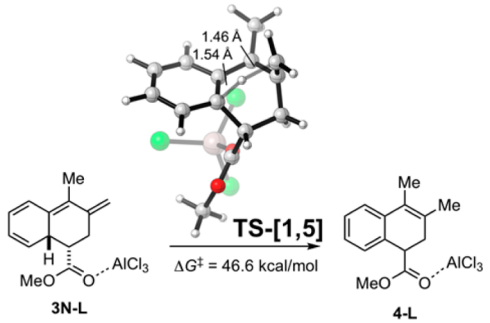

Figure 7. Transition structure for the concerted [1,5]-H shift.

distorted and has a computed barrier of 46.6 kcal/mol. We think it is likely a stepwise proton transfer process assisted by anionic species such as Cl^- or $AlCl_4^-$ in the reaction mixture.

Chirality Transfer and the Origins of Stereoselectivity. Modest transfer of chirality was observed when chiral arylallene (*R*)-**6** was used (Scheme 2), although the absolute stereochemistry of the major product was unknown. We have modeled this process and predicted (*S*)-7 to be the major product. The results are shown in Figure 8.

Scheme 2. Diels–Alder Reaction of Chiral Allene (*R*)-6 and Methyl Acrylate (2)[12]

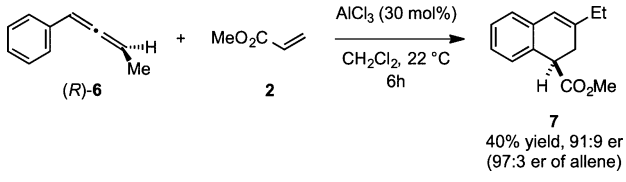

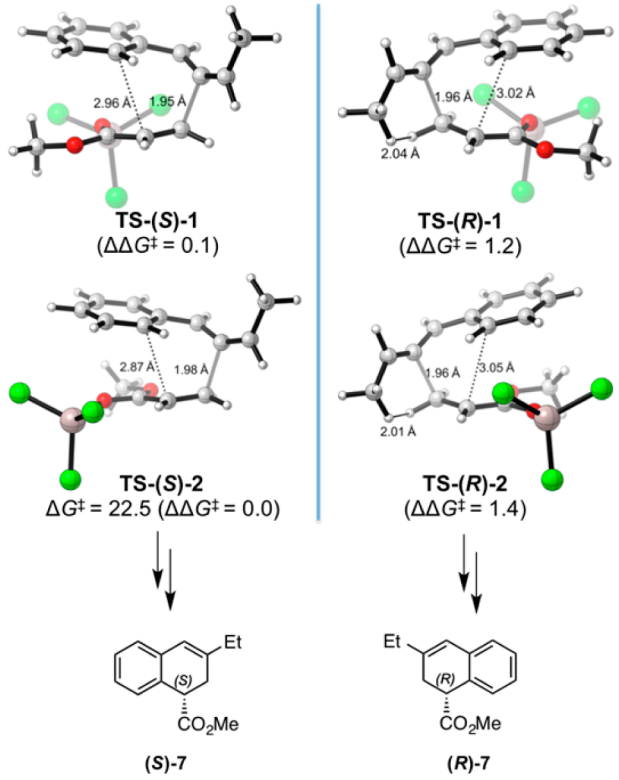

Figure 8. Lowest energy transition structures and the corresponding products for the Diels–Alder reaction of chiral allene (*R*)-**6**.

The four transition structures are all *endo*, with TS-(*S*)-1 and TS-(*S*)-2 (different conformations of acrylate) leading to (*S*)-7, and TS-(*R*)-1 and TS-(*R*)-2 leading to (*R*)-7. The transition structures leading to (*R*)-7 are disfavored due to the steric clashes between the methyl hydrogen of the allene and the alkene hydrogen of the acrylate (2.04 and 2.01 Å as shown in Figure 8). This unfavorable interaction is absent in the transition structures leading to (*S*)-7. The computed $\Delta\Delta G^{\ddagger}$ values agree well with the experimentally measured enantiomeric ratio of the two products, and (*S*)-7 is predicted to be the major one.

CONCLUSION

The Lewis acid-catalyzed Diels–Alder reactions of arylallenes and acrylates involve stepwise mechanisms in which short-lived zwitterion intermediates are formed. The reaction is *endo*-selective in the presence of Lewis acid catalyst. The [2 + 2] cycloaddition is not observed because of the greater charge separation in the first step of the [2 + 2] cycloaddition. The limited substrate scope of the dienophiles is due to the greater distortion energies to bend the carbon–X bond, where X is a non-hydrogen β-substituent on the acrylate. This is a result of the highly asynchronous nature of the transition structure in the stepwise mechanism of this Diels–Alder reaction. We have predicted the absolute stereochemistry of the product of the Diels–Alder reaction using chiral arylallenes and identified the origins of the observed stereoselectivity.

ASSOCIATED CONTENT

Supporting Information

The Supporting Information is available free of charge on the ACS Publications website at DOI: 10.1021/acs.joc.7b01132.

DOI: 10.1021/acs.joc.7b01132
J. Org. Chem. 2017, 82, 6398–6402

Additional computational results and coordinates and energies of the stationary points (PDF)

AUTHOR INFORMATION

Corresponding Author

*E-mail: houk@chem.ucla.edu.

ORCID

Peiyuan Yu: 0000-0002-4367-6866

K. N. Houk: 0000-0002-8387-5261

Author Contributions

†P.Y. and W.L. contributed equally to this work.

Notes

The authors declare no competing financial interest.

ACKNOWLEDGMENTS

We are grateful to the National Science Foundation (Grant CHE-1361104) for financial support of this research. Calculations were performed on the Hoffman2 cluster at the University of California, Los Angeles, and the Extreme Science and Engineering Discovery Environment (XSEDE), which is supported by the National Science Foundation (Grant OCI-1053575).

REFERENCES

(1) Diels, O.; Alder, K. *Justus Liebigs Ann. Chem.* **1928**, *460*, 98.

(2) Norton, J. A. *Chem. Rev.* **1942**, *31*, 319.

(3) Martin, J. G.; Hill, R. K. *Chem. Rev.* **1961**, *61*, 537.

(4) Winkler, J. D. *Chem. Rev.* **1996**, *96*, 167.

(5) Nicolaou, K. C.; Snyder, S. A.; Montagnon, T.; Vassilikogiannakis, G. *Angew. Chem., Int. Ed.* **2002**, *41*, 1668.

(6) (a) Blackman, M. L.; Royzen, M.; Fox, J. M. *J. Am. Chem. Soc.* **2008**, *130*, 13518. (b) Devaraj, N. K.; Weissleder, R.; Hilderbrand, S. A. *Bioconjugate Chem.* **2008**, *19*, 2297.

(7) (a) Hoye, T. R.; Baire, B.; Niu, D.; Willoughby, P. H.; Woods, B. P. *Nature* **2012**, *490*, 208. (b) Yun, S. Y.; Wang, K.-P.; Lee, N.-K.; Mamidipalli, P.; Lee, D. *J. Am. Chem. Soc.* **2013**, *135*, 4668. (c) Liang, Y.; Hong, X.; Yu, P.; Houk, K. N. *Org. Lett.* **2014**, *16*, 5702. (d) Yu, P.; Yang, Z.; Liang, Y.; Hong, X.; Li, Y.; Houk, K. N. *J. Am. Chem. Soc.* **2016**, *138*, 8247.

(8) Newton, C. G.; Drew, S. L.; Lawrence, A. L.; Willis, A. C.; Paddon-Row, M. N.; Sherburn, M. S. *Nat. Chem.* **2015**, *7*, 82.

(9) Aragonès, A. C.; Haworth, N. L.; Darwish, N.; Ciampi, S.; Bloomfield, N. J.; Wallace, G. G.; Diez-Perez, I.; Coote, M. L. *Nature* **2016**, *531*, 88.

(10) Li, L.; Yu, P.; Tang, M.-C.; Zou, Y.; Gao, S.-S.; Hung, Y.-S.; Zhao, M.; Watanabe, K.; Houk, K. N.; Tang, Y. *J. Am. Chem. Soc.* **2016**, *138*, 15837.

(11) (a) Qiu, H.; Srinivas, H.; Zavalij, P.; Doyle, M. P. *J. Am. Chem. Soc.* **2016**, *138*, 1808. (b) Duan, A.; Yu, P.; Liu, F.; Qiu, H.; Gu, F. L.; Doyle, M. P.; Houk, K. N. *J. Am. Chem. Soc.* **2017**, *139*, 2766.

(12) Conner, M. L.; Brown, M. K. *Tetrahedron* **2016**, *72*, 3759.

(13) (a) Conner, N. K.; Xu, Y.; Brown, M. K. *J. Am. Chem. Soc.* **2015**, *137*, 3482. (b) Rasik, C. M.; Brown, M. K. *Angew. Chem., Int. Ed.* **2014**, *53*, 14522. (c) Rasik, C. M.; Hong, Y. J.; Tantillo, D. J.; Brown, M. K. *Org. Lett.* **2014**, *16*, 5168. (d) Rasik, C.; Brown, M. *Synlett* **2014**, *25*, 760.

(14) Houk, K. N.; Strozier, R. W. *J. Am. Chem. Soc.* **1973**, *95*, 4094.

(15) Frisch, M. J.; Trucks, G. W.; Schlegel, H. B.; Scuseria, G. E.; Robb, M. A.; Cheeseman, J. R.; Scalmani, G.; Barone, V.; Mennucci, B.; Petersson, G. A.; Nakatsuji, H.; Caricato, M.; Li, X.; Hratchian, H. P.; Izmaylov, A. F.; Bloino, J.; Zheng, G.; Sonnenberg, J. L.; Hada, M.; Ehara, M.; Toyota, K.; Fukuda, R.; Hasegawa, J.; Ishida, M.; Nakajima, T.; Honda, Y.; Kitao, O.; Nakai, H.; Vreven, T.; Montgomery, J. A., Jr.; Peralta, J. E.; Ogliaro, F.; Bearpark, M.; Heyd, J. J.; Brothers, E.; Kudin, K. N.; Staroverov, V. N.; Kobayashi, R.; Normand, J.; Raghavachari, K.; Rendell, A.; Burant, J. C.; Iyengar, S. S.; Tomasi, J.; Cossi, M.; Rega, N.; Millam, M. J.; Klene, M.; Knox, J. E.; Cross, J. B.; Bakken, V.; Adamo, C.; Jaramillo, J.; Gomperts, R.; Stratmann, R. E.; Yazyev, O.; Austin, A. J.; Cammi, R.; Pomelli, C.; Ochterski, J. W.; Martin, R. L.; Morokuma, K.; Zakrzewski, V. G.; Voth, G. A.; Salvador, P.; Dannenberg, J. J.; Dapprich, S.; Daniels, A. D.; Farkas, Ö.; Foresman, J. B.; Ortiz, J. V.; Cioslowski, J.; Fox, D. J. *Gaussian 09*, revision D.01; Gaussian, Inc.: Wallingford, CT, 2013.

(16) (a) Zhao, Y.; Truhlar, D. G. *Theor. Chem. Acc.* **2008**, *120*, 215. (b) Zhao, Y.; Truhlar, D. G. *Acc. Chem. Res.* **2008**, *41*, 157.

(17) (a) Barone, V.; Cossi, M. *J. Phys. Chem. A* **1998**, *102*, 1995. (b) Cossi, M.; Rega, N.; Scalmani, G.; Barone, V. *J. Comput. Chem.* **2003**, *24*, 669.

(18) Zhao, Y.; Truhlar, D. G. *Phys. Chem. Chem. Phys.* **2008**, *10*, 2813.

(19) Legault, C. Y. *CYLview*, version 1.0b; Université de Sherbrooke: Sherbrooke, Canada, 2009; http://www.cylview.org.

(20) Dennington, R.; Keith, T.; Millam, J. *GaussView*, version 5; Semichem Inc.: Shawnee Mission, KS, 2009.

(21) (a) Avogadro: an open-source molecular builder and visualization tool, version 1.1.1. http://avogadro.openmolecules.net/. (b) Hanwell, M. D.; Curtis, D. E.; Lonie, D. C.; Vandermeersch, T.; Zurek, E.; Hutchison, G. R. *J. Cheminf.* **2012**, *4*, 17.

(22) Yang, Z.; Yu, P.; Houk, K. N. *J. Am. Chem. Soc.* **2016**, *138*, 4237.

(23) (a) Ess, D. H.; Houk, K. N. *J. Am. Chem. Soc.* **2007**, *129*, 10646. (b) Fernández, I.; Bickelhaupt, F. M. *Chem. Soc. Rev.* **2014**, *43*, 4953. The distortion/interaction or activation strain model has been used to study the reactivity and selectivity of a variety of cycloaddition reactions. For recent examples, see: (c) Yang, Y.-F.; Liang, Y.; Liu, F.; Houk, K. N. *J. Am. Chem. Soc.* **2016**, *138*, 1660. (d) Lin, B.; Yu, P.; He, C. Q.; Houk, K. N. *Bioorg. Med. Chem.* **2016**, *24*, 4787. (e) Fernández, I.; Bickelhaupt, F. M. *Chem. - Asian J.* **2016**, *11*, 3297.

DOI: 10.1021/acs.joc.7b01132
J. Org. Chem. 2017, 82, 6398−6402